Galvanomagnetic Investigation of Energy Bands in Arsenic*

J. R. SYBERT, H. J. MACKEY, AND K. L. HATHCOX
Department of Physics, North Texas State University, Denton, Texas
(Received 5 October 1967)

The isothermal magnetoresistivity and Hall resistivity in a monocrystal of arsenic have been studied at temperatures of liquid helium in fields up to 25 kG. All measurements were taken in the basal plane of the crystal with magnetic field perpendicular to the plane and parallel to the trigonal axis. The binary axis was in the basal plane and parallel to the long dimension of the crystal. The magnetoconductivity tensor element σ_{11} and the Hall conductivity element σ_{12} were constructed from resistivity data and analyzed in terms of two- and three-band models. A least-squares curve fitting of the conductivities to the quasiclassical model of Sondheimer and Wilson indicates two major energy bands of carriers. The Hall effect is positive. The high-mobility carriers are holes with mobility approximately four times that of the equally populous electrons. The carrier concentration is $n \simeq 2\times10^{20}/\text{cm}^3$ if determined from σ_{11} data along with effective-mass anisotropy data established from quantum-oscillation studies. Simultaneous curve fitting of the σ_{11} and σ_{12} data gives $n \simeq 0.7\times10^{20}/\text{cm}^3$.

I. INTRODUCTION

As a means of studying the energy-band structure of arsenic, galvanomagnetic potentials have been measured in fields ranging to 25 kG and at temperatures of liquid helium. The magnetoresistance and Hall effect both exhibit quantum oscillations (Shubnikov–de Haas effect) at the coldest temperatures.[1] The gross conductivities, upon which the Shubnikov–de Haas effect oscillations are superimposed, have been analyzed to determine various parameters characterizing the energy bands in arsenic. This paper concerns the analysis of data relating to the gross effects.

The general problem of galvanomagnetic determination of electron energy-band structure in metals is quite extensive, involving, for crystals with the $3\bar{m}$ symmetry of arsenic, simultaneous determination of 12 independent resistivity tensor components to second order in magnetic field. Difficulty in utilizing an exact algebraic solution to the 12 independent equations generally leads one to a curve-fitting technique for a reasonable determination of the resistivity (or conductivity) components. Additionally, sample preparation can be a major problem as at least two samples, different in orientation but identical in composition, are required.

As a good approximate technique we utilize a modification of the theory of electrical conductivities by Sondheimer and Wilson,[2] and express the electrical conduction properties of arsenic in terms of a few simple parameters. Additional parameters may be obtained by combining results of the modified Sondheimer-Wilson analysis with arsenic Fermi-surface parameters obtained from quantum-oscillation experiments.

The first detailed investigation of the electronic structure of arsenic was carried out by Berlincourt, employing the de Haas–van Alphen effect.[3] Quite recently, the Fermi surface and energy-band structure of arsenic have been examined by various techniques: The phenomena studied include de Haas–van Alphen effect,[4,5] ultrasonic attenuation,[5,6] de Haas–Shubnikov effect,[1] specific heat,[7,8] and cyclotron resonance.[9] Also, an oscillatory magnetothermal effect has recently been observed in arsenic.[10] Theoretical considerations[11] yield a model for the Fermi surface consistent with that proposed from the most recent de Haas–van Alphen studies. Many parameters relating to the Fermi surface have yet to be accurately determined, but the recently proposed model seems quite reasonable, and subject to perhaps only small modification. It will be seen that the galvanomagnetic data is compatible with the model, yielding numerical values for several parameters in reasonable agreement with those obtained from studies of the quantum oscillations.

Specifically, isothermal electrical conductivities have been measured in a transverse magnetic field and the data interpreted in terms of the Sondheimer–Wilson theory. This theory and related information will be outlined in Sec. II. A brief discussion relating to the monocrystalline sample follows in Sec. III. In Sec. IV detailed results of this experimental investigation are given, and in so doing the findings are related to existing information on the Fermi surface in arsenic.

* Supported in part by a grant from the U. S. Department of Army, No. DAHC 15-67-G2, administered through the Southwest Center for Advanced Studies, Dallas, Tex.

[1] J. R. Sybert, H. J. Mackey, and R. E. Miller, Phys. Letters **24A**, 655 (1967).
[2] A. H. Wilson, *The Theory of Metals* (Cambridge University Press, Cambridge, England, 1959).
[3] T. G. Berlincourt, Phys. Rev. **99**, 1716 (1955).
[4] J. Vanderkooy and W. R. Datars, Phys. Rev. **156**, 671 (1967).
[5] Y. Shapira and S. J. Williamson, Phys. Letters **14**, 73 (1965).
[6] J. B. Ketterson and Y. Eckstein, Phys. Rev. **140**, A1355 (1965).
[7] Harvey V. Culbert, Bull. Am. Phys. Soc. **10**, 1104 (1965); Phys. Rev. **157**, 560 (1967).
[8] William A. Taylor, D. C. McCollum, B. C. Passenheim, and H. W. White, Phys. Rev. **161**, 652 (1967).
[9] C. S. Ih and D. N. Langenberg, Bull. Am. Phys. Soc. **11**, 402 (1966).
[10] S. Noguchi and S. Tanuma, Phys. Letters **24A**, 710 (1967).
[11] P. J. Lin and L. M. Falicov, Phys. Rev. **142**, 441 (1966).

II. MODIFIED SONDHEIMER–WILSON THEORY

The isothermal-transport effects are represented in kinetic theory by the expression

$$\mathbf{J}=\boldsymbol{\sigma}\cdot\mathbf{E}^*, \tag{1}$$

where $\mathbf{J}$ is the electric-current density, $\boldsymbol{\sigma}$ is the conductivity tensor, and $\mathbf{E}^*$ is the electric field. The notation is for the special case of isothermal conditions, derived from more general transport equations discussed in earlier publications.[12,13] The experimentally determined coefficients of magnetoresistivity $\rho_{11}=E_x^*/J_x$ and Hall resistivity $\rho_{21}=E_y^*/J_x$, measured with current in the binary direction and magnetic field along the trigonal direction, are related to the elements of the conductivity tensor by

$$\sigma_{11}=\rho_{11}/(\rho_{11}^2+\rho_{12}^2),$$
$$\sigma_{12}=\rho_{21}/(\rho_{11}^2+\rho_{21}^2). \tag{2}$$

The element σ_{11} is the magnetoconductivity and σ_{12} is the Hall conductivity.

The monotonic parts of σ_{11} and σ_{12} are analyzed in terms of a modified Sondheimer–Wilson theory.[2] Here, one assumes a quasicontinuum of states in "parabolic" bands with sharp Fermi distribution functions and isotropic relaxation times independent of energy. The resulting expressions are

$$\sigma_{11}=ec\sum a_i n_i H_i L_i,$$
$$\sigma_{12}=ec\sum(\pm)n_i L_i H, \tag{3}$$

where the summation extends over all bands. The (+) sign is for holes and (−) for electrons. In the above Eq. (3), $H_i=(\alpha_i\alpha_2)^{-1/2}c/e\tau_i$ is a quantity inversely proportional to the mobility at zero field and is called the saturation field; α_1 and α_2 are elements of the inverse effective-mass tensor, τ_i is the relaxation time, n_i is the carrier concentration, and L_i is the Lorentz factor:

$$L_i=(H^2+H_i^2)^{-1}.$$

The factor a_i is introduced to correct for noncircular orbits of the carriers; $a_i=1$ for circular orbits, while for the tilted ellipsoids applicable to the problem at hand, it is most simply expressed in terms of the reciprocal effective-mass-tensor elements[13,14]:

$$a_i=\tfrac{1}{2}[(\alpha_1/\alpha_2)^{1/2}+(\alpha_2/\alpha_1)^{1/2}]. \tag{4}$$

(The tilted-ellipsoid expression for a_i is somewhat more complicated when written in terms of the elements of the effective-mass tensor $\mathbf{m}^*$.[13])

Equation (3) is expected to be a good approximation for low fields. It will be seen that the expressions are quite applicable over the entire range of 25 kG covered in this experiment. In the analysis which follows, experimental data for the magnetic-field dependence of σ_{12} and σ_{11} will be fitted to Eqs. (3). The data is fitted by a least-squares technique,[15] varying the parameters H_i, $a_i n_i$, and n_i. In this manner it is possible to obtain numerical values for the partial mobilities $\mu_i=1/H_i$, carrier concentrations, and eccentricities of the Fermi ellipsoids (given the angle of tilt obtained from quantum-oscillation experiments).

III. EXPERIMENTAL DETAILS

Arsenic is a semimetal with the same rhombohedral crystal structure as the other semimetals bismuth and antimony. (Expected similarities in electronic structure of arsenic and other semimetals will be noted in Sec. IV.) The coordinate system used in the discussion is shown in Fig. 1. The x, y, z axes coincide with the binary, bisectrix, and trigonal axis of the crystal, respectively. In all experiments relating to the gross-conductivity measurements, the magnetic field was directed along the z axis, electric current along the x axis. Hall probes sampled the electric field E_y, and magnetoresistance probes measured E_x.

The arsenic monocrystal was grown in the form of a right parallelepiped (16.6×8.2×1.6 mm) by Semi-Elements, Inc. The resistivity ratio was of the order of $\rho^{300°}/\rho^{4.2°}\simeq 200$. After temperature cycling of the arsenic crystal, repeated measurements of the resistivity ratio gave values in the range $149<\rho^{300°}/\rho^{1.90°}<207$. It is interesting to note that variations of this order in the

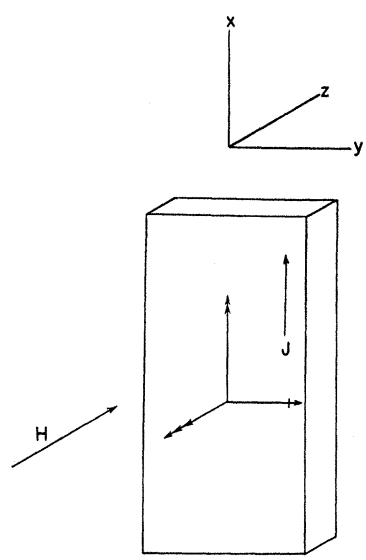

FIG. 1. The arsenic crystal and its symmetry axes. All data were taken with magnetic field $\mathbf{H}$ oriented along the trigonal axis. Electric current $\mathbf{J}$ was along the x axis (binary direction). The bisectrix coincides with the y axis.

[12] C. G. Grenier, J. M. Reynolds, and N. H. Zebouni, Phys. Rev. 129, 1088 (1963).
[13] C. G. Grenier, J. M. Reynolds, and J. R. Sybert, Phys. Rev. 132, 58 (1963).
[14] G. N. Rao, N. H. Zebouni, C. G. Grenier, and J. M. Reynolds, Phys. Rev. 133, A141 (1964).
[15] H. J. Mackey, Ph.D. dissertation, Louisiana State University, 1963 (unpublished).

resistivity ratio are not at all uncommon in bismuth.[16–18] Electrical probes were soldered to the crystal with 30/70 lead-tin solder. Ohmic contact was obtained relatively easily, although mechanical stability of the junctions was sometimes a problem. A straightforward dc technique was employed. The voltages to be measured were fed directly to a Honeywell six-dial thermal-free microvolt potentiometer, the off-balance of which was amplified by a Keithley model 147 nanovolt null detector and fed through a voltage divider to a strip chart recorder. Calibration and voltage bias were obtained from the microvolt potentiometer. The noise level was approximately 3 nV under optimum conditions.

IV. RESULTS AND DISCUSSION

A. Model for the Arsenic Fermi Surface

A reasonably detailed model of the Fermi surface has been suggested theoretically by the pseudopotential band-structure calculation of Lin and Falicov[11] and experimentally by the de Haas–van Alphen studies of Priestley *et al.*[19] The proposed model is quite similar to the multiple-ellipsoid surface observed by various investigators in Sb.[14,20] For purposes of analysis in terms of a small number of simple parameters the model is taken in the multiellipsoid approximation.

Specifically, the electron Fermi surface consists of three ellipsoids with major axis lying within 6° of the basal plane (x-y plane). The primary ellipsoid has one principal axis along the binary direction and the major principal axis tilted a few degrees from the basal plane toward the trigonal axis.

This principal ellipsoid is represented by the expression

$$2m_0\zeta^\beta=\beta_1p_x^2+\beta_2p_y^2+\beta_3p_z^2+2\beta_4p_yp_z. \quad (5a)$$

The remaining two nonprincipal ellipsoids are obtained by $\pm120°$ rotation about the trigonal axis and are given by

$$2m_0\zeta^\beta=\tfrac{1}{4}(\beta_1+3\beta_2)p_x^2+\tfrac{1}{4}(3\beta_1+\beta_2)p_y^2+\beta_3p_z^2 \pm\tfrac{1}{2}\sqrt{3}(\beta_1-\beta_2)p_xp_y\pm\sqrt{3}\beta_4p_xp_z-\beta_4p_yp_z. \quad (5b)$$

With this notation, the β_i are elements of the tensor $\boldsymbol{\beta}=m_0\mathbf{m}^{*-1}$, where $\mathbf{m}^{*-1}$ is the inverse effective-mass tensor; $\boldsymbol{\beta}$ has the form

$$=\begin{bmatrix}\beta_1 & 0 & 0\\ 0 & \beta_2 & \beta_4\\ 0 & \beta_4 & \beta_3\end{bmatrix}.$$

The Fermi surface for holes is described in exactly the same manner simply by replacing α_i for β_i and ζ^α for ζ^β. de Haas–van Alphen results indicate a multiply connected six-ellipsoid surface for the holes. In that which follows the six-ellipsoid model is used and the connecting surface is either neglected or accounted for (in a rough manner) by considering it to be an additional parabolic band of carriers.

Values for the elements of the inverse effective-mass tensors $\boldsymbol{\alpha}$ and $\boldsymbol{\beta}$ have been inferred from results of quantum-oscillation studies.[1,6,19] These are given in Table I along with resulting values for the anisotropy factor a_i.

TABLE I. Inverse effective-mass tensor elements and anisotropy factors for the α and β carriers (tilted ellipsoids).

	$(m_0/m)_1$	$(m_0/m)_2$	$(m_0/m)_3$	$(m_0/m)_4$	a_i
$\boldsymbol{\alpha}$	7.72	9.12	5.48	6.53	1.004
$\boldsymbol{\beta}$	6.10	0.66	10.13	1.07	1.685

B. Experimental Results

Band Fit to σ_{11}

Results of the three-band fit for the magnetoconductivity σ_{11} as a function of magnetic field are shown in Figs. 2 and 3. Table II gives the values of parameters obtained from the least-squares fit to the data.

The values of n_1 and n_2, for the α holes and the β electrons, respectively, have been calculated using the a_i from Table I. The a_i for the α holes is assigned to the high-mobility band (Band I) since the high-mobility carriers are seen to have positive sign from σ_{12} band fittings. Note that the values of carrier concentrations deduced in this manner are in general agreement with values reported by others.[3,6] The conductivity is governed almost entirely by the first two bands, α holes and β electrons, respectively. Contribution of the third band is almost insignificant. This is verified by a two-band fit to the same experimental data. The temperature dependence of the H_i is not in the expected direction. The small variation in the H_i values is extremely dependent upon the relative weight given the experimental points in the least-squares curve fit. Here the experimental points have been taken equally spaced in H on a logarithmic scale, with equal weight assigned to the points. A different weighting of the points does give

TABLE II. Energy-band parameters determined from σ_{11} curves. Three-band fit.

	(1)	(2)	(3)
	$T=1.19°$K		
H_i (G)	579	1595	8803
a_in_i (10^{20}/cm^3)	2.46	2.93	0.241
n_i (10^{20}/cm^3)	2.45	1.74	···
	$T=4.2°$K		
H_i (G)	523	1437	8397
a_in_i (10^{20}/cm^3)	1.52	3.36	0.238
n_i (10^{20}/cm^3)	1.51	1.99	···

[16] R. N. Zitter, Phys. Rev. **127**, 1471 (1962).
[17] Allen N. Friedman, Phys. Rev. **159**, 553 (1967).
[18] B. J. Vaughn, M.S. thesis, North Texas State University, 1967 (unpublished).
[19] M. G. Priestley, L. R. Windmiller, J. B. Ketterson, and Y. Eckstein, Phys. Rev. **154**, 671 (1967).
[20] Lee R. Windmiller, Phys. Rev. **149**, 472 (1966).

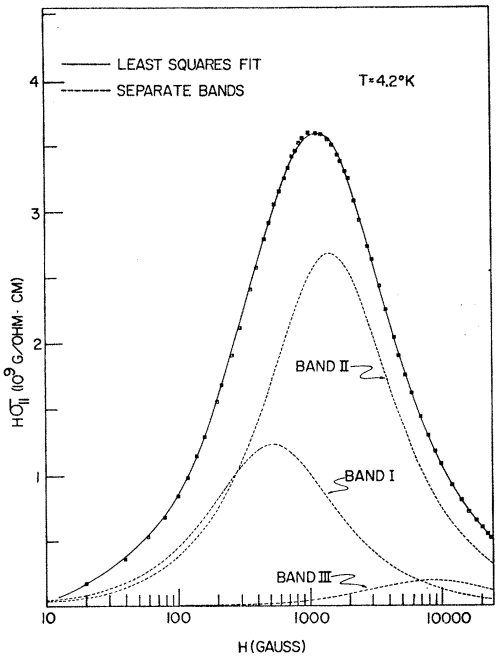

FIG. 2. Three-band curve fit to the σ_{11} data at 4.2°K. The individual bands (dashed curves) add to give the least-squares fit to σ_{11}. Representative experimental points are shown. The quantum oscillations which are superimposed on the experimental resistivity data have been removed by graphical techniques.

the expected increase of the H_i's with temperature. However, due to the sensitivity of the H_i's to the weighting of the experimental points, and the small variation of H_i from 1.19 to 4.2°K, it is not reasonable

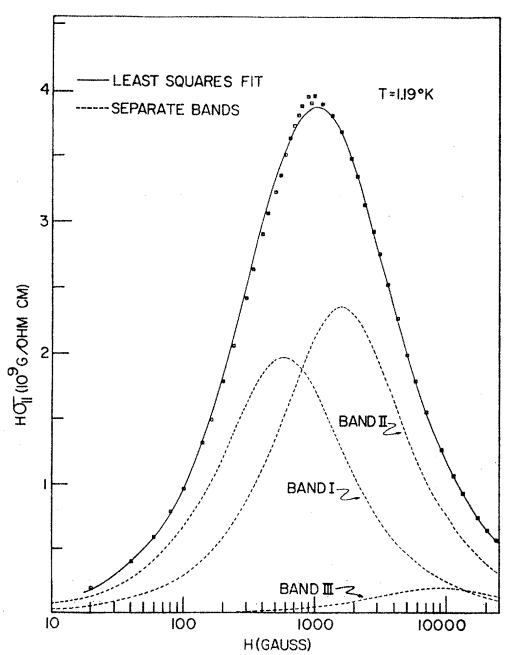

FIG. 3. Three-band curve fit to the σ_{11} data at 1.19°K. Characteristics are essentially the same as Fig. 2.

TABLE III. Energy-band parameters determined from σ_{12} curves.

	Two-band fit (1)	Two-band fit (2)	Three-band fit (1)	Three-band fit (2)	Three-band fit (3)
		$T=1.19$°K			
H_i (G)	...	...	69	418	2462
n_i (10^{20}/cm^3)	...	...	0.009	0.478	−0.483
		$T=4.2$°K			
H_i (G)	464	2172	472	2060	10930
n_i (10^{20}/cm^3)	0.538	−0.533	0.554	−0.541	−0.013

to attempt an analysis of the temperature dependence by this technique. Note, however, that from the values of the elements of $\boldsymbol{\alpha}$ and $\boldsymbol{\beta}$ given in Table I, and assuming approximately equal relaxation times for the α holes and β electrons, one expects a ratio $H_2/H_1 \simeq 4.2$. Values of H_2/H_1 ranging from 3 to 4 are obtained, in rough agreement with the expected value. Relaxation times calculated from the data of Tables I and II give $\tau \approx 10^{-10}$ sec in the liquid-helium range of temperatures.

Band Fit to σ_{12} Data

Experimental data for the Hall isothermal conductivity are given in Table III and displayed in Fig, 4. Again, there are two predominant bands, identified by their algebraic sign as α holes and β electrons, the carriers of highest mobility (lowest H_i value) being the α holes. Saturation field values are essentially the same as in the σ_{11} data, but the carrier concentrations are a

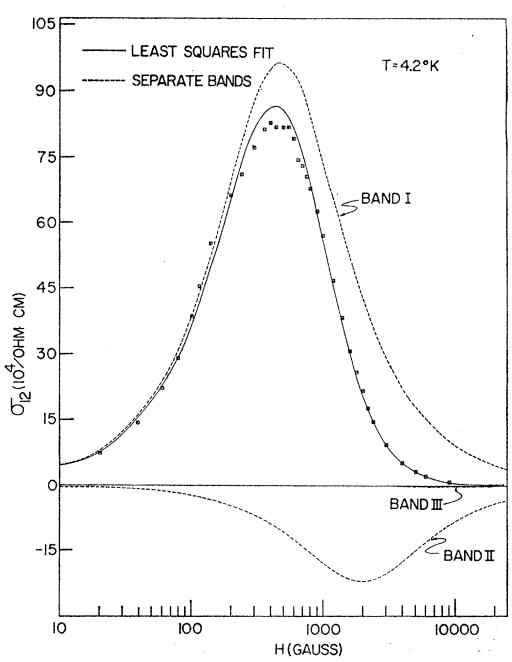

FIG. 4. Three-band curve fit to the σ_{12} data at 4.2°K. Band I is identified as the α holes with the almost equally populous (but lower-mobility) band II corresponding to the β electrons. The contribution of band III is insignificant.

factor of 3 smaller than expected from magnetoconductivity results alone. Inclusion of a third band has little effect upon the results, and must be considered quite insignificant in the conduction process. At 1.19°K, the third band appears as holes of high mobility, whereas the 4.2°K data give the third band as low-mobility electrons. In either case, the carrier concentration and contribution of the band to the total conductivity is quite small and could be considered as resulting simply from small experimental inaccuracies in the resistivity data.

Two-Band Simultaneous Fit of σ_{11} and σ_{12}

It has been observed in the preceding discussion that the two major energy bands account for almost all of the σ_{11} and σ_{12} effects. In terms of the simplified theory (with isotropic relaxation time τ) the saturation fields H_i for a given band of carriers appearing in the σ_{12} and the σ_{11} curves should be identical. With this in mind, a simultaneous fit to the σ_{12} and σ_{11} curves has been made, requiring that each curve fitting have the same value for H_1 and also for H_2. No restriction has been placed upon the numerator factors involving carrier concentrations. Figures 5 and 6 show the results of the two-band simultaneous fit at 4.2°K. Table IV lists the energy-band parameters obtained from the curve fitting and corresponding to the figures.[21] Upon inspection of Tables IV and V, one again observes features which are characteristic of the individual curve fittings: The expected increase in the H_i with increasing temperature is not established, but the ratio $H_2/H_1 \simeq 4$. The σ_{11} data for $n_i a_i$ are of the same order as those obtained from the individual fit and, using independently determined values for a_i, yield values for carrier concentrations in close agreement with quantum-oscillation experiments. The n_i as determined from the Hall conductivity are very close to the values obtained from the individual σ_{12} curve fit. The a_i are approximately three times larger than those given in Table I.

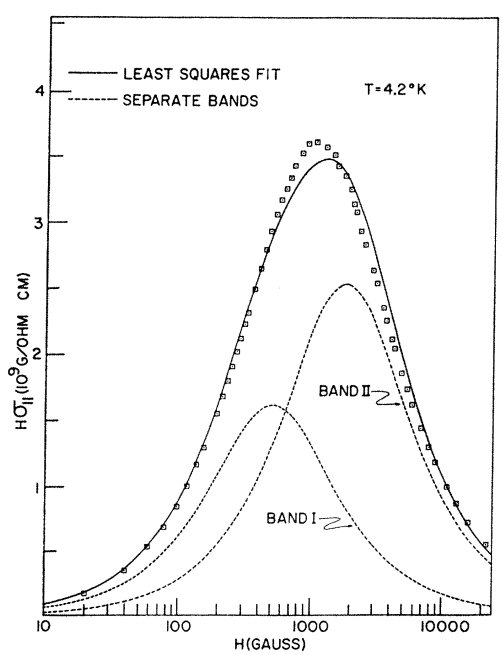

FIG. 5. Magnetoconductivity portion of simultaneous two-band fit at 4.2°K. Curve fit to the experimental points is substantially poorer than the corresponding individual three-band σ_{11} curve fit of Fig. 2.

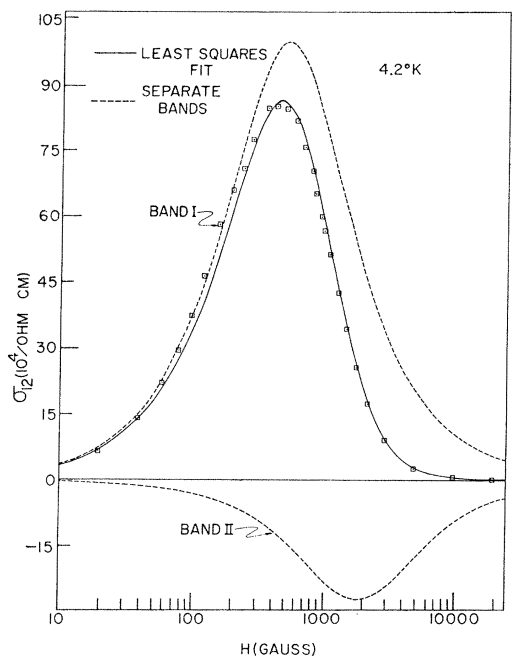

FIG. 6. Hall conductivity portion of simultaneous two-band curve fit at 4.2°K. Band I contains the α holes and band II corresponds to the β electrons.

Three-Band Simultaneous Fit

Inclusion of a third band gives, as in the case of the individual curve fittings, a closer fit to the experimental data. However, one can see from Table V that the search routine has found it necessary to split the α band developed in the two-band fit into two separate bands in order to work with a three-band model. Taken at face value, the numerical results are anomalous with respect to the results of all the other curve fits. But if one coalesces the two α bands into one whose parameters are here designated by primes, the following approxi-

[21] The simultaneous curve fitting was performed on the CDC 6600 at Los Alamos Scientific Laboratory. A slightly different weighting of the experimental points was used here in order to effect a reduction in the average percent error of the curve fitting.

TABLE IV. Energy-band parameters obtained from a simultaneous fit for σ_{11} and σ_{12} at 4.2°K.

	Two-band fit (1)	Two-band fit (2)	Three-band fit (1)	Three-band fit (2)	Three-band fit (3)
H_i (G)	521	1880	537	1502	6750
$a_i n_i$ (10^{20}/cm^3)	2.01	3.12	1.73	3.11	0.26
n_i (10^{20}/cm^3)	0.650	−0.644	0.738	−0.675	−0.061
a_i	3.09	4.84	2.34	4.60	4.26

mate values are obtained:

$$H_1' \simeq \tfrac{1}{2}(H_1+H_2)=516\,,$$
$$a_1 n_1' \simeq (a_1 n_1 + a_2 n_2)=3.57\,,$$
$$n_1' \simeq (n_1+n_2)=0.548\,,$$
$$a_1' \simeq (a_1' n_1')/n_1'=6.51\,.$$

Comparison of these rough values to the results of the two-band fit indicates that the formation of two α bands at low field is indeed just due to a splitting of the α band of the two-band fit in an attempt to minimize the total error. The weight of the total evidence supports the view that the actual presence of a third band of carriers cannot be resolved, because of the experimental inaccuracies inherent in the measurement of the small, but critical, low-field data.

Resistivities

Reconstructions of the ρ_{21} and ρ_{11} from the σ_{12} and σ_{11} curve fits of Figs. 2 and 4 are shown in Figs. 7 and 8. The curve, reconstructed by inverting the $\boldsymbol{\sigma}$ tensor and using the established energy-band parameters, is seen to follow the experimental points quite closely for all ranges of magnetic field. (It is interesting to note that the Sondheimer–Wilson theory has no magnetic-field dependence in ρ_{11} for a single spherical band.)

V. CONCLUSIONS

The data and analysis of the preceding section lead to the following conclusions concerning the electron energy-band structure of arsenic:

(a) The carriers with highest mobility are holes as determined from the σ_{12} band fittings. The band-structure calculations of Lin and Falicov[11] indicate quasiellipsoidal surfaces of holes with large tilt from the basal plane. Quantum-oscillation experiments[6,19] have shown these large-tilt carriers. As may be seen

TABLE V. Energy-band parameters obtained from a simultaneous fit for σ_{11} and σ_{12} at 1.19°K.

	Two-band fit (1)	Two-band fit (2)	Three-band fit (1)	Three-band fit (2)	Three-band fit (3)
H_i (G)	470	1916	292	741	2415
$a_i n_i$ (10^{20}/cm^3)	2.26	3.32	0.235	3.33	2.05
n_i (10^{20}/cm^3)	0.631	−0.621	0.272	0.276	−0.528
a_i	3.58	5.31	0.86	12.06	3.88

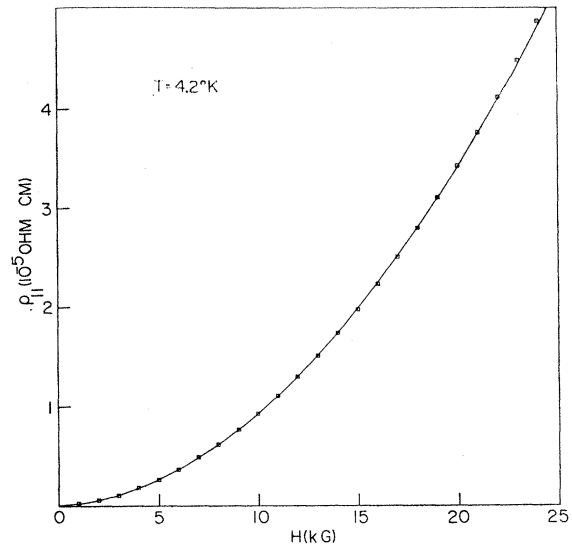

FIG. 7. Reconstruction of the magnetoresistivity from data shown in Figs. 2 and 4. The solid curve is the ρ_{11} indicated by the least-squares fittings to σ_{11} and σ_{12} of Figs. 2 and 4, respectively. Representative experimental points are shown in close agreement with the reconstructed curve.

from Eq. (4), the a_i is a measure of the eccentricity of the ellipse formed by the intersection of the basal plane and the tilted ellipsoid. Therefore, the large-tilt hole ellipsoids should have a smaller value of a_i than the small-tilt electron ellipsoids. Results of band fittings as shown in Tables IV and V give $a_1 < a_2$. Thus, the high-mobility holes (Band I) are identified as the large-tilt carriers of Lin and Falicov.[11]

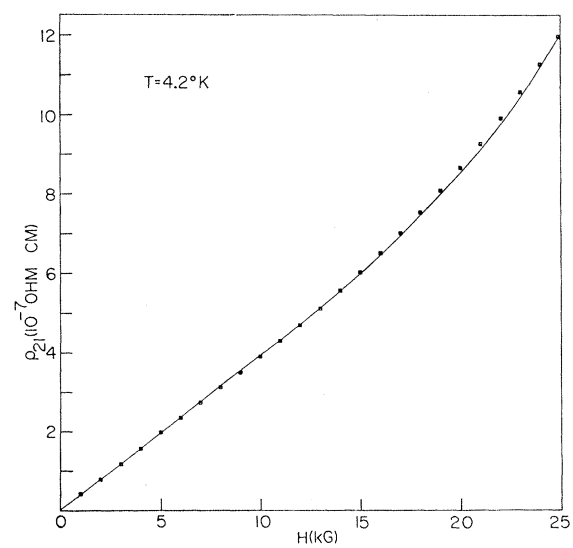

FIG. 8. Reconstruction of the Hall resistivity from data shown in Figs. 2 and 4. The solid curve is the ρ_{21} indicated by the least-squares fittings to σ_{11} and σ_{12} of Figs. 2 and 4, respectively. Experimental points are in close agreement with the least-squares curve.

(b) The carriers of lower mobility (large H_i) are electrons, again in agreement with theory and quantum-oscillation experiments. Concentration of these electrons (β carriers) is substantially the same as for the α holes.

(c) A third band of carriers with concentration an order of magnitude less than the α and β carriers is possible, but not strongly indicated by the experimental data. (It is of interest to note that when a four-band fit was attempted for the conductivity data, two of the bands coalesced into a single band, thereby reducing the results to a three-band fit.)

(d) Using established values for elements of the reciprocal effective-mass tensor, the σ_{11} data give values of carrier concentration which are in quite good agreement with results of quantum-oscillation experiments. However, the self-consistent results of σ_{11} and σ_{12} curve fitting give values of n_i a factor of 3 smaller than those expected from σ_{11} data alone. Correspondingly, experimentally determined anisotropy factors a_i are about three times larger than expected, which would be difficult to reconcile with the almost irrefutable measurements of periods in quantum-oscillation phenomena.

(e) The band fittings indicate that $H_2/H_1 \simeq 4$. Using the mass-tensor elements of Table I, this ratio indicates $\tau_\alpha \simeq \tau_\beta \simeq 10^{-10}$ sec.

(f) The Sondheimer–Wilson curve fittings show two major bands quite clearly, but the technique is not applicable to the problem of determining further detailed parameters of energy bands of relatively low-carrier concentration. The Sondheimer–Wilson technique, applied to arsenic, gives values of carrier concentration of the same order but somewhat lower than values of n_i obtained from quantum-oscillation experiments. (The same techniques, applied to the semimetals bismuth and antimony, give values of n_i in much closer agreement to quantum-oscillation results.[13,14])

ACKNOWLEDGMENT

The authors are indebted to Dr. Jonas T. Holdemann, Jr., of the Los Alamos Scientific Laboratory for performing some of the least-squares calculations using his search routine on the CDC 6600.

PHYSICAL REVIEW VOLUME 166, NUMBER 3 15 FEBRUARY 1968

Galvanomagnetic Studies in Metals by Means of Heliconlike Waves*

JOHN R. MERRILL†
Laboratory of Atomic and Solid State Physics, Cornell University, Ithaca, New York
(Received 25 August 1967)

This paper delineates the materials in which magnetoplasma waves in metals can be used to measure elements of the resistivity tensor. Results from the noble metals and from Al and In are discussed. The strengths and weaknesses of the wave method are discussed and compared with standard direct-current experimental methods. The magnetoplasma wave which was used is called the helicon in simple isotropic solids and is called the Whistler wave in ionospheric physics. The agreement between measurements of the anisotropy of resistivity tensor elements in copper as measured by this heliconlike-wave technique and those made by dc magnetoresistivity studies is very good.

INTRODUCTION

FOR many years, dc measurements of galvanomagnetic effects have been used to help determine Fermi-surface topology in metals.[1] While the magnetoresistivity has been the most widely used galvanomagnetic effect, the Hall effect and transverse even voltage have also been used to measure properties of the microscopic behavior of electronic carriers.[2] This paper concerns measurements of galvanomagnetic coefficients by means of the low-frequency magnetoplasma wave. In isotropic, uncompensated materials, this wave is known as the helicon.[3] The paper concerns measurements of the anisotropic propagation of helicon waves in single crystals of such materials as Cu, Ag, Au, Al, and In. We find that these wave measurements of the dependence of the diagonal and off-diagonal resistivity tensor elements upon crystallographic orientation agree very well with dc measurements in those

* This work was supported by the U. S. Atomic Energy Commission under Contract No. AT(30-1)-2150, NYO-2150-37, and by the Advanced Research Projects Agency through the Materials Science Center at Cornell University.

† Present address: Department of Physics and Astronomy, Dartmouth College, Hanover, N. H.

[1] I. M. Lifshitz, M. I. Azbel, and M. I. Kaganov, Zh. Eksperim. i Teor. Fiz. **31**, 63 (1956) [English transl.: Soviet Phys.—JETP **4**, 41 (1957)]; E. Fawcett, Advan. Phys. **13**, 139 (1964).

[2] J. R. Klauder, W. A. Reed, G. F. Brennert, and J. E. Kunzler, Phys. Rev. **141**, 592 (1966).

[3] R. Bowers, in *Proceedings of the Symposium on Plasma Effects in Solids, Paris, 1964* (Academic Press Inc., New York, 1965), p. 19; S. J. Buchsbaum, *ibid.*, p. 3.